



(11) **EP 4 029 500 A1**

(12) **EUROPEAN PATENT APPLICATION**

(43) Date of publication:  
**20.07.2022 Bulletin 2022/29**

(21) Application number: **21382025.1**

(22) Date of filing: **15.01.2021**

(51) International Patent Classification (IPC):  
**A61K 31/404** <sup>(2006.01)</sup> **A61P 35/00** <sup>(2006.01)</sup>  
**A61K 31/407** <sup>(2006.01)</sup> **A61P 25/14** <sup>(2006.01)</sup>  
**A61P 31/04** <sup>(2006.01)</sup>

(52) Cooperative Patent Classification (CPC):  
**A61K 31/404; A61K 31/407; A61P 1/16**

(84) Designated Contracting States:  
**AL AT BE BG CH CY CZ DE DK EE ES FI FR GB  
GR HR HU IE IS IT LI LT LU LV MC MK MT NL NO  
PL PT RO RS SE SI SK SM TR**  
Designated Extension States:  
**BA ME**  
Designated Validation States:  
**KH MA MD TN**

(71) Applicants:

- **Universidad Autónoma de Madrid**  
28049 Madrid (ES)
- **Consejo Superior De Investigaciones Científicas**  
28006 Madrid (ES)
- **Universidad Miguel Hernández de Elche**  
03202 Elche, Alicante (ES)
- **Fundación para la Investigación Biomédica del Hospital Universitario La Princesa**  
28006 Madrid (ES)

(72) Inventors:

- **CUADRADO PASTOR, Antonio**  
28029 Madrid (ES)

- **FERNÁNDEZ GINÉS, Raquel**  
28029 Madrid (ES)
- **ENCINAR, José Antonio**  
03202 Elche (ES)
- **LEÓN MARTÍNEZ, Rafael**  
28006 Madrid (ES)
- **FRANCO GONZÁLEZ, Juan Felipe**  
28040 Madrid (ES)
- **GARCÍA LÓPEZ, Manuela**  
28029 Madrid (ES)
- **RODRÍGUEZ FRANCO, María Isabel**  
28006 Madrid (ES)
- **ROJO SANCHÍS, Ana Isabel**  
28029 Madrid (ES)

(74) Representative: **Hoffmann Eitle**  
**Hoffmann Eitle S.L.U.**  
Paseo de la Castellana 140, 3a planta  
Edificio LIMA  
28046 Madrid (ES)

(54) **TETRAHYDRO-SPIROINDOLINE-PYRROLOPYRROLE-TRIONES INHIBITORS OF THE NRF2-BETA-TRCP INTERACTION FOR USE IN THE TREATMENT OF NRF2-RELATED DISEASES**

(57) The present invention relates to NRF2- $\beta$ TrCP interaction inhibitors for use in the treatment of NRF2-related diseases.

**EP 4 029 500 A1**

## Description

### FIELD OF THE INVENTION

**[0001]** The present invention is comprised in the medical field. Particularly, the present invention relates to NRF2- $\beta$ TrCP interaction inhibitors, for use in the treatment of NRF2-related diseases.

### STATE OF THE ART

**[0002]** Inflammatory response plays an important role in the pathology of most diseases. In clinical practice, there is a large number of non-steroidal anti-inflammatory drugs (NSAIDs) for alleviating pain and inflammation. However, NSAIDs have adverse side effects whose risk of onset is higher the higher the dose and/or the longer the duration over time. Irritation of the digestive tract, hepatotoxicity, high blood pressure, fluid retention, kidney problems, heart problems, and/or rashes are included among the unwanted side effects which may occur.

**[0003]** There is therefore an unresolved medical need to find other compounds that may perform an anti-inflammatory and cytoprotective function without exhibiting the side effects described in the preceding paragraph.

**[0004]** Precisely for the purpose of solving said technical problem, compounds with these properties have been developed in the present invention based on the activation of NRF2 (nuclear factor (erythroid-derived 2)-like 2) transcription factor by means of a novel technique consisting of interrupting the interaction thereof with the E3 ligase adaptor protein referred to as  $\beta$ TrCP (beta-transducin repeat-containing E3 ubiquitin protein ligase).

### DESCRIPTION OF THE INVENTION

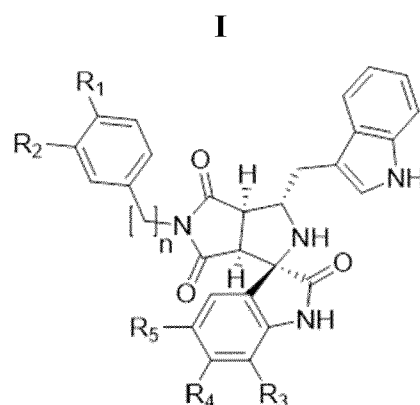
#### Brief Description of the Invention

**[0005]** As indicated above, the present invention relates to NRF2- $\beta$ TrCP interaction inhibitors for use in the treatment of NRF2-related diseases (see **Figure 1**).

**[0006]** In this sense, it must be pointed out that NRF2-related diseases belong to a defined and limited group of diseases identified in the general knowledge of the subject. By way of example, document [Antonio Cuadrado, et al., 2018. Transcription Factor NRF2 as a Therapeutic Target for Chronic Diseases: A Systems Medicine Approach. *Pharmacological Reviews* April 2018, 70(2)348-383; DOI: <https://doi.org/10.1124/pr.117.014753>] relates to disruptions of the NRF2 interactome in several diseases. According to this document, a map of 37 NRF2-related diseases has been developed based on DisGeNET (Pinero et al., 2017) and GeneCards (Stelzer et al., 2016) databases, as well as knowledge from some studies in animal models. In this document, disease-gene associations for these pathologies have also been retrieved using Dis-

GeNET, OMIM, and GWAS databases (Menche et al., 2015). The interactome-based proximity (Guney and Oliva, 2014) of NRF2 to known disease genes for each of the NRF2-related disease phenotypes is shown in Figure 4 of this document. NRF2 is significantly closer to the known disease genes of the digestive system and cancers, such as prostate cancer, liver cancer, and lung neoplasms, compared with randomly selected proteins, highlighting the key functional role of NRF2 in these pathologies. Moreover, NRF2 was found to be proximal to various proteins related to metabolic and cardiovascular diseases, such as diabetes, hyperglycemia, ischemia, middle cerebral artery infarction, and atherosclerosis. Protein interactions of NRF2 also connect it to genes associated with respiratory disorders such as asthma, pulmonary fibrosis, and pulmonary emphysema, as well as neurodegenerative diseases such as multiple sclerosis, Alzheimer's disease (AD), Parkinson's disease (PD), amyotrophic lateral sclerosis (ALS), and Friedreich's ataxia. Particularly, this group of diseases includes: autoimmune diseases (multiple sclerosis, asthma, vitiligo, lupus erythematosus, rheumatoid arthritis); chronic respiratory diseases (fibrosis or pulmonary emphysema, COPD: chronic obstructive pulmonary disease); cardiovascular diseases (atherosclerosis, high blood pressure, middle cerebral artery infarction, ischemia); diseases of the digestive system (inflammatory bowel disease, liver fibrosis, NASH: nonalcoholic steatohepatitis, cirrhosis); metabolic diseases (type 2 diabetes mellitus, hyperglycemia); neurodegenerative diseases (Alzheimer's disease, Parkinson's disease, amyotrophic lateral sclerosis, Friedreich's ataxia), and cancer. Furthermore, the invention is also applicable to certain infectious diseases occurring with a high level of oxidative stress and inflammation.

**[0007]** Therefore, the first aspect of the present invention relates to NRF2- $\beta$ TrCP interaction inhibitors, characterized by Formula (I), or its derivative salts,



wherein:

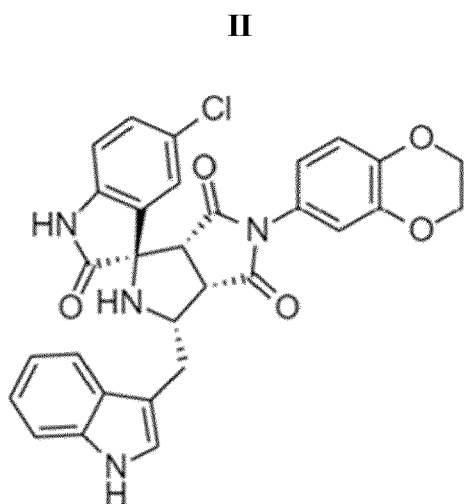
- **n** can be 0 or 1,
- **R<sub>1</sub>** can be O<sub>2</sub>CCH<sub>3</sub> or a six-membered ring for forming a benzodioxane, benzomethylenedioxy, or naph-

thalene substituent;

- $R_2$  can be H or a six-membered ring for forming a benzodioxane, benzomethylenedioxy, or naphthalene substituent;
- $R_3$  can be H or  $CH_3$ ;
- $R_4$  can be H or  $CH_3$ ; and
- $R_5$  can be H, Cl, or  $CH_3$ .

for use in the treatment of NRF2-related diseases.

**[0008]** In a preferred aspect of the invention, the NRF2- $\beta$ TrCP interaction inhibitor is characterized by Formula (II) (hereinafter also referred to as PHAR),



or its derivative salts.

**[0009]** The second aspect of the present invention relates to a pharmaceutical composition comprising the NRF2- $\beta$ TrCP interaction inhibitor of Formula I or II, or derivative salts thereof, and optionally pharmaceutically acceptable vehicles or excipients, for use in the treatment of NRF2-related diseases. Alternatively, the present invention relates to a method for the treatment of NRF2-related diseases comprising the administration of a therapeutically effective dose or amount of a pharmaceutical composition comprising the NRF2- $\beta$ TrCP interaction inhibitor of Formula I or II, or derivative salts thereof.

**[0010]** In a preferred aspect, the invention relates to said NRF2- $\beta$ TrCP interaction inhibitors for use in the treatment of an NRF2-related disease caused by inflammation and oxidative stress.

**[0011]** In a preferred aspect, the invention relates to said NRF2- $\beta$ TrCP interaction inhibitors for use in the treatment of a disease caused by Gram-negative bacterial infection.

**[0012]** The third aspect of the present invention relates to an *in vitro* method for identifying and producing compounds for the treatment of NRF2-related diseases, which comprises: a) determining if the inhibition of NRF2- $\beta$ TrCP interaction by the candidate compound has taken place, and b) wherein if the inhibition of NRF2- $\beta$ TrCP interaction has taken place, it is indicative of the selected

compound being effective in the treatment of NRF2-related diseases.

**[0013]** In a preferred aspect, the present invention relates to an *in vitro* method for identifying and producing compounds for the treatment of NRF2-related diseases caused by inflammation and oxidative stress, which comprises: a) determining if the inhibition of NRF2- $\beta$ TrCP interaction by the candidate compound has taken place, and b) wherein if the inhibition of NRF2- $\beta$ TrCP interaction has taken place, it is indicative of the selected compound being effective in the treatment of NRF2-related diseases caused by inflammation and oxidative stress.

**[0014]** In a preferred aspect, the present invention relates to an *in vitro* method for identifying and producing compounds for the treatment of a disease caused by Gram-negative bacterial infection, which comprises: a) determining if the inhibition of NRF2- $\beta$ TrCP interaction by the candidate compound has taken place, and b) wherein if the inhibition of NRF2- $\beta$ TrCP interaction has taken place, it is indicative of the selected compound being effective in the treatment of a disease caused by Gram-negative bacterial infection.

**[0015]** Different approaches have been used to determine if the compound inhibits said interaction:

1. First, the PI3K/AKT signaling pathway is inhibited, and therefore GSK-3 $\beta$  is activated with the PI3K inhibitor, LY294002. As a result, NRF2 is phosphorylated by GSK-3 $\beta$  and marked for degradation by means of interaction with  $\beta$ -TrCP. Therefore, if PHAR is capable of inhibiting  $\beta$ -TrCP-NRF2 interaction, the NRF2 levels will remain stable independently of the activation and phosphorylation by GSK-3 $\beta$ . The obtained result corroborates this.
2. Using MEFs derived from NRF2 knock-in mice (Nrf2-2Ki) developed by the present group. In this model, serines 335 and 338, which are fundamental for interaction with  $\beta$ -TrCP, have been substituted with alanines. In this manner, GSK-3 $\beta$  cannot phosphorylate NRF2, and therefore a protein which is not recognized by  $\beta$ -TrCP, and which, accordingly, should also not be sensitive to the action of PHAR, is generated. Therefore, PHAR-mediated NRF2 activation was considerably lower in Nrf2-2Ki MEFs compared with WT MEFs.
3. Using lentiviral silencing of the two isoforms described for  $\beta$ -TrCP ( $\beta$ -TrCP1 and  $\beta$ -TrCP2) in MEFs originating from Keap1 knockout mice (Keap1 $^{-/-}$ ). Even though the silencing achieved was not 100%, NRF2 and HO-1 induction was considerably lower in  $\beta$ -TrCP-silenced cells compared with shCTRL cells.

**[0016]** The following terms are defined for a better interpretation of the present invention:

- "NRF2-related diseases": are a specific group of diseases characterized in that the patients suffering

same present an altered expression or activity of NRF2. This group of diseases is also known with the term NRF2 diseasome [Antonio Cuadrado, et al., 2018. Transcription Factor NRF2 as a Therapeutic Target for Chronic Diseases: A Systems Medicine Approach. *Pharmacological Reviews* April 2018, 70(2)348-383; DOI: <https://doi.org/10.11241/pr.117.014753>]. Particularly, this group of diseases includes: autoimmune diseases (multiple sclerosis, asthma, vitiligo, lupus erythematosus, rheumatoid arthritis); chronic respiratory diseases (fibrosis or pulmonary emphysema, COPD: chronic obstructive pulmonary disease); cardiovascular diseases (atherosclerosis, high blood pressure, middle cerebral artery infarction, ischemia); diseases of the digestive system (inflammatory bowel disease, liver fibrosis, NASH: non-alcoholic steatohepatitis, cirrhosis); metabolic diseases (type 2 diabetes mellitus, hyperglycemia); neurodegenerative diseases (Alzheimer's disease, Parkinson's disease, amyotrophic lateral sclerosis, Friedreich's ataxia), and cancer. Furthermore, the invention is also applicable to certain infectious diseases occurring with a high level of oxidative stress and inflammation.

- The term "comprising" means including but not limited to what follows the word "comprising". Therefore, the use of the term "comprising" indicates that the listed elements are compulsory, but that other elements are optional and may or may not be present.
- "Consists of" is understood as including and not limited to everything following the phrase "consists of". Therefore, the phrase "consists of" indicates that the listed elements are compulsory, and that there can be no other elements present.
- "Therapeutically effective dose or amount" is understood as the amount which, when administered as described herein, produces a positive therapeutic response in a subject suffering from the disease. The exact amount required will vary from one subject to another, depending on the age and general condition of the subject, the severity of the condition being treated, the mode of administration, and the like. A suitable "effective" amount in any individual case can be determined by a person skilled in the art using routine experimentation, based on the information provided herein.

## Description of the Figures

[0017]

**Figure 1. NRF2 structure.** The different NRF2 domains are shown. The low affinity and high affinity motifs recognized by KEAP1 for interacting with NRF2 are shown in detail in the Neh2 domain. The moieties for GSK-3 $\beta$  interaction and the possible

phosphorylation sites of (a) priming kinase(s) which is/are unknown at present are shown in the Neh6 domain.

**Figure 2. Computational methodology carried out in this study.** Diagram of the experiment carried out for identifying new candidate  $\beta$ -TrCP and NRF2 protein-protein interaction inhibitors.

**Figure 3. PHAR binds specifically to  $\beta$ -TrCP but not to KEAP1. A) and B),** structure of the  $\beta$ -TrCP complex (PDB:1P22) with the lowest free energy PHAR conformation. The figures illustrate the  $\beta$ -TrCP moieties participating in hydrophobic or electrostatic intermolecular interactions, respectively, with pNRF2, compared with the moieties for interaction with PHAR.  $\beta$ -TrCP is shown in a representation referred to as cartoon. Color code: Yellow: specific moieties for pNRF2/ $\beta$ -TrCP interaction; magenta: specific moieties for PHAR/ $\beta$ -TrCP interaction; blue: moieties shared between PHAR/pNRF2 and  $\beta$ -TrCP. **C) and D),** molecular dynamics simulations of PHAR with respect to  $\beta$ -TrCP and KEAP1 proteins, respectively, at a study time of 100 ns.  $\beta$ -TrCP and KEAP1 are shown in surface representation. **E),** map showing the interaction of  $\beta$ -TrCP moieties which interact with pNRF2 and/or PHAR throughout the 100 ns of the molecular dynamics simulation. The distance of interaction is represented by a color code in which black corresponds with the closest moieties and yellow the farthest ones. **F),** chemical absorption, distribution, metabolism, excretion, and toxicity (ADMET) properties of PHAR. MW: molecular weight; H-Acceptors: hydrogen bond acceptors; H-Donors: hydrogen bond donors; cLogS: estimated log (base 10) of solubility measured in mol/L; cLogP: estimated log (base 10) of n-octanol/water partition coefficient; Ro5violations: violations of Lipinski's rule of five; BBB: blood-brain barrier permeation capacity; Caco-2 permeab.: Caco-2 permeability; and HIA: human intestinal absorption was calculated using the web application DataWarrior and the ADMETSar online tool.

**Figure 4. PHAR activates the NRF2 pathway.** MEFs in serum-poor conditions were subjected to **(A-C)** 1  $\mu$ M, 3  $\mu$ M, or 10  $\mu$ M of PHAR and 10  $\mu$ M of SFN as a positive control for 16 h; or **(D-F)** 10  $\mu$ M of PHAR for the indicated times. In both experiments, 0.1% DMSO was used as a vehicle. **A),** representative immunoblots of NRF2, HO1, KEAP1, LAMINB, and GAPDH as loading controls. **B) and C),** densitometric analysis of NRF2 and HO1 protein levels of the representative immunoblots depicted in **(A)**, expressed as a ratio of NRF2/LAMINB or HO1/GAPDH. The data is depicted as means  $\pm$  SEM (n = 3). Statistical analysis was performed with one-way ANOVA followed by the Bonferroni test to check in-

ter-group differences. \* $p < 0.05$ ; \*\*\* $p < 0.001$  vs. 0. **D**), representative immunoblots of NRF2, HO1, KEAP1, LAMINB, and GAPDH as loading controls. **E** and **F**), Densitometric analysis of NRF2 and HO1 protein levels of the representative immunoblots of **(D)**, expressed as a ratio of NRF2/LAMINB or HO1/GAPDH. The data is depicted as means  $\pm$  SEM (n = 3). Statistical analysis was performed with one-way ANOVA followed by the Bonferroni test to check inter-group differences. \* $p < 0.05$ ; \*\*\* $p < 0.001$  vs. 0. **G**, MCF-7 c32 ARE-luc were subjected to 1  $\mu$ M, 3  $\mu$ M, or 10  $\mu$ M of PHAR and 10  $\mu$ M of SFN as a positive control. 0.1% DMSO was used as a vehicle. Luciferase activity was measured after 16 h of treatment. The data is depicted as means  $\pm$  SEM (n = 3). Statistical analysis was performed with one-way ANOVA followed by the Bonferroni test to check inter-group differences. \*\* $p < 0.01$ ; \*\*\* $p < 0.001$  vs. 0. **H**), MTT assay to evaluate cell viability/toxicity after treatments. **I**), Serum-poor MEFs were subjected to 10  $\mu$ M of PHAR. The mRNA levels of *Hmox1*, *Nqo1*, *Aox1*, *Gclc*, and *Gclm* after 8 h of treatment were determined by means of pRT-PCR and normalized by means of average *LaminB*, *Gapdh*, and  *$\beta$ -actin*. The data is depicted as means  $\pm$  SEM (n = 3). Statistical analysis was performed with the Student's T test. \* $p < 0.05$ ; \*\* $p < 0.01$  \*\*\* $p < 0.001$  vs. 0.

**Figure 5. PHAR-mediated NRF2 activation is independent of KEAP1 and said activation is responsible for the increase in the expression of its targets. (A-D)** Serum-deprived MEFs originating from wild-type (WT) or KEAP1 null (*Keap1*<sup>-/-</sup>) mice treated with 10  $\mu$ M of PHAR for the indicated times. 0.1% DMSO was used as a vehicle. **A**), representative immunoblots of NRF2, HO1, KEAP1, LAMINB, and GAPDH as loading controls. **B**) and **C**), densitometric analysis of NRF2 and HO1 protein levels of the representative immunoblots of **(A)**, expressed as a ratio of NRF2/LAMINB or HO1/GAPDH. The data is depicted as means  $\pm$  SEM (n = 3). Statistical analysis was performed with two-way ANOVA followed by the Bonferroni test to check inter-group differences. **D**), the mRNA levels of *Hmox-1*, *Nqo1*, *Aox1*, *Gclc*, and *Gclm* were determined after 8 h of 10  $\mu$ M PHAR by means of qRT-PCR and normalized by means of average *Gapdh*, *Tbp*, and  *$\beta$ -actin*. The data is depicted as mean  $\pm$  SEM (n = 3). Statistical analysis was performed with two-way ANOVA followed by the Bonferroni test to check inter-group differences. \* $p < 0.05$ ; \*\* $p < 0.01$ ; \*\*\* $p < 0.001$  vs. 0 of MEF-WT. **(E-H)**, Serum-deprived MEFs from wild-type (WT) or NRF2 null (*Nrf2*<sup>-/-</sup>) mice were subjected to 10  $\mu$ M of PHAR for the indicated times. 0.1% DMSO was used as a vehicle. **E**), representative immunoblots of NRF2, HO1, KEAP1, LAMINB, and GAPDH as loading controls. **F**) and **G**), densitometric analysis of NRF2 and HO1 protein levels of the rep-

resentative immunoblots of **(E)**, expressed as a ratio of NRF2/LAMINB or HO 1/GAPDH. The data is depicted as means  $\pm$  SEM (n = 3). Statistical analysis was performed with two-way ANOVA followed by the Bonferroni test to check inter-group differences. \* $p < 0.05$ ; \*\* $p < 0.01$ ; p\*\*\* $< 0.001$  vs. MET WT. **H**), the mRNA levels of *Hmox-1*, *Nqo1*, *Aox1*, *Gclc*, and *Gclm* were determined after 8h of 10  $\mu$ M PHAR by means of qRT-PCR and normalized by means of average *Gapdh*, *Tbp*, and  *$\beta$ -actin*. The data is depicted as mean  $\pm$  SEM (n = 3). Statistical analysis was performed with two-way ANOVA followed by the Bonferroni test to check inter-group differences. \* $p < 0.05$ ; \*\* $p < 0.01$ ; \*\*\* $p < 0.001$  vs. MEF-WT.

**Figure 6. PHAR increases NRF2 protein levels in a  $\beta$ -TrCP-dependent manner. (A and B)** Serum-deprived MEFs from KEAP1 null mice (*Keap1*<sup>-/-</sup>) were treated with 10  $\mu$ M of PHAR for 60 min. 0.1% DMSO was used as a vehicle. The cells were then treated with 20  $\mu$ M of LY294002 for the indicated times. **A**), representative immunoblots of NRF2, pSer473-AKT, AKT, pS9-GSK3, GSK3, KEAP1, and GAPDH as loading controls. **B**), densitometric analysis of NRF2 protein levels of the representative immunoblot of **(A)**, expressed as a ratio of NRF2/GAPDH. The data is depicted as means  $\pm$  SEM (n = 3). Statistical analysis was performed with two-way ANOVA followed by the Bonferroni test to compare inter-group differences. \* $p < 0.05$  vs. LY294002. **C**), MEFs originating from wild-type mice (WT) and MEFs originating from serum-poor NRF2 knock-in mice (*Nrf2-2Ki*) were treated with different doses of PHAR (1  $\mu$ M, 3  $\mu$ M, and 9  $\mu$ M) and 10  $\mu$ M of SFN used as a positive control for 16h. **C**), representative immunoblots of NRF2, HO1, and  $\beta$ ACTIN as a loading control (n= 1). **(D-H)**, MEF originating from *Keap1*<sup>-/-</sup> mice were transduced with a lentivirus encoding mouse shCTRL or anti- $\beta$ -TrCP1/2 sh. The serum-deprived MEFs were subjected to 10  $\mu$ M of PHAR for the indicated times. 0.1% DMSO was used as a vehicle. **D**), representative immunoblots of NRF2,  $\beta$ -CATENIN, HO1, KEAP1, and GAPDH as loading controls. **E**) and **F**), densitometric analysis of NRF2 and HO1 protein levels of the representative immunoblots of **(D)**, expressed as a ratio of NRF2 and HO1/GAPDH. The data is depicted as means  $\pm$  SEM (n = 3). Statistical analysis was performed with two-way ANOVA followed by the Bonferroni test to check inter-group differences. \*\* $p < 0.01$ ; \*\*\* $p < 0.001$  vs. shCTRL. **G**) and **H**), the mRNA levels of  *$\beta$ -TrCP1*,  *$\beta$ -TrCP2*, *Hmox-1*, and *Nqo1* were determined by means of qRT-PCR and normalized by means of average *Gapdh*, *Tbp*, and  *$\beta$ -actin*. The data is depicted as mean  $\pm$  SEM (n = 3). Statistical analysis was performed with two-way ANOVA followed by the Bonferroni test to check inter-group differences. \*\*\* $p < 0.001$  vs. shCTRL.

### Figure 7. PHAR reduces inflammatory response

**in LPS-stimulated Raw264.7 cells.** Serum-deprived Raw264.7 cells were pretreated with 10  $\mu$ M of PHAR for 8 h. 0.1% DMSO was used as a vehicle. After that period of time, the cells were treated with 100 ng/ml of LPS for the indicated times. **A**), representative immunoblots of NRF2, HO1, p65, pre-IL1 $\beta$ , COX2, NOS2, and GAPDH as a loading control. The black arrow tip marks the specific band of p65 and NOS2. **B**), densitometric analysis of HO1 and NRF2 protein levels of the representative immunoblots of **(A)**, expressed as a ratio of protein/GAPDH levels. The data is depicted as means  $\pm$  SEM (n = 3). Statistical analysis was performed with two-way ANOVA followed by the Bonferroni test to compare inter-group differences. \*\*\*p < 0.001 vs LPS. **C**), Densitometric analysis of pre-IL1 $\beta$ , COX2, and NOS2 protein levels of the representative immunoblots of **(A)**, expressed as a ratio of protein/GAPDH levels. The data is depicted as means  $\pm$  SEM (n = 3). Statistical analysis was performed with two-way ANOVA followed by the Bonferroni test to compare inter-group differences. \*\*\*p < 0.001 vs. LPS. **D**) and **E**), the mRNA levels of *Il1 $\beta$* , *Cox2*, *Nos2*, *Il6*, and *Tnf $\alpha$*  were determined by means of qRT-PCR and normalized by means of average *Gapdh*, *Tbp*, and  *$\beta$ -actin*. The data is depicted as mean  $\pm$  SEM (n = 3). Statistical analysis was performed with two-way ANOVA followed by the Bonferroni test to check inter-group differences. \*\*\*p < 0.001 vs. LPS.

### Figure 8. PHAR reduces inflammatory response in peritoneal macrophages originating from *Nrf2*<sup>+/+</sup> mice but not in peritoneal macrophages originating from LPS-stimulated *Nrf2*-4KI mice.

Peritoneal macrophages originating from wild-type (WT) and serum-deprived NRF2 *knock-in* (*Nrf2*-4KI) mice were pretreated with 10  $\mu$ M of PHAR for 8 h. 0.1% DMSO was used as a vehicle. After that period of time, the cells were treated with 100 ng/ml of LPS for 4 h. **A**), representative immunoblots originating from both cell types of NRF2, HO1, pre-IL1 $\beta$ , COX2, NOS2, and GAPDH as a loading control. **B**), densitometric analysis of NRF2 and HO1 protein levels of the representative immunoblots of **(A)**, expressed as a ratio of protein/GAPDH levels. The data is depicted as means  $\pm$  SEM (n = 3). Statistical analysis was performed with two-way ANOVA followed by the Bonferroni test to compare inter-group differences. \*p < 0.05; \*\*p < 0.01; \*\*\*p < 0.001 vs. LPS. **C**), Densitometric analysis of pre-IL1 $\beta$ , COX2, and NOS2 protein levels of the representative immunoblots of **(A)**, expressed as a ratio of protein/GAPDH levels. The data is depicted as means  $\pm$  SEM (n = 3). Statistical analysis was performed with two-way ANOVA followed by the Bonferroni test to compare inter-group differences. \*p < 0.05; \*\*p < 0.01; \*\*\*p < 0.001 vs. LPS. **D**), the mRNA levels of *Hmox1*, *Il1 $\beta$* , *Cox2*, *Nos2*,

*Il6*, and *Tnf $\alpha$*  were determined by means of qRT-PCR and normalized by means of average *Gapdh*, *Tbp*, and  *$\beta$ -actin*. The data is depicted as mean  $\pm$  SEM (n = 3). Statistical analysis was performed with two-way ANOVA followed by the Bonferroni test to check inter-group differences. \*p < 0.05; \*\*p < 0.01; \*\*\*p < 0.001 vs. LPS.

### Figure 9. PHAR activates NRF2 and HO-1 in liver.

**A**), UV and MS spectrum derived from the HPLC-MS analysis of PHAR dissolved in methanol for the identification of peaks associated with the compound. A blue rectangle surrounds the mass associated with PHAR. **(B-D)**, the mice were treated with the vehicle (Tween-80 + PBS, 1:13), 50 mg/kg of PHAR, or 50 mg/kg of SFN (saline) as a positive control by means of intraperitoneal (IP) injection for 2 hours. **B**), HPLC-MS UV and MS spectra derived from representative liver samples of both experimental groups used for determining PHAR levels in the liver 120 min after a single IP injection of 50 mg/kg. A blue rectangle surrounds the mass associated with PHAR. **C**), representative immunoblots showing NRF2, HO1, and LAMINB protein levels as the liver extract loading control. **D**), densitometric analysis of NRF2 protein levels of the representative immunoblots shown in **(C)**, expressed as a ratio of NRF2/LAMINB. Statistical analysis was performed with one-way ANOVA followed by the Bonferroni test to compare inter-group differences. \*\*\*p < 0.001 vs. vehicle. **E**) and **F**), the mice were treated daily with vehicle (Tween-80 + PBS, 1:13) or 50 mg/kg of PHAR by means of intraperitoneal injection for 5 days. **E**), representative immunoblots showing NRF2, HO1, and LAMINB protein levels as the liver extract loading control. **F**), densitometric analysis of NRF2 and HO1 protein levels in the liver tissue of the representative immunoblots shown in **(E)**, expressed as a ratio of NRF2/LAMINB or HO1/LAMINB levels. Statistical analysis was performed with one-way ANOVA followed by the Bonferroni test to compare inter-group differences. \*\*p < 0.01 vs. vehicle.

### Figure 10. PHAR reduces inflammatory response in LPS-treated mice.

The mice were divided into 4 experimental groups (n=4). Experimental groups 1 and 3 were treated by IP route with vehicle (Tween-80 + PBS, 1:13) and experimental groups 2 and 4 with 50 mg/kg of PHAR for 5 days. After the second-to-last administration of the compound, groups 3 and 4 were treated by IP route with 1 mg/kg of LPS for 24 h. Two hours after the last dose of PHAR and twenty-four hours after the administration of LPS, all the mice were sacrificed by extracting the liver protein and total RNA, **A**), representative immunoblots showing NRF2, HO1, and GAPDH protein levels as the liver extract loading control. **B**), densitometric analysis of NRF2 and HO1 protein levels of the rep-

representative immunoblots shown in **(A)**, expressed as a ratio of NRF2/GAPDH or HO1/GAPDH. The data is depicted as means  $\pm$  SEM ( $n = 4$ ). Statistical analysis was performed with one-way ANOVA followed by the Bonferroni test to compare inter-group differences.  $**p < 0.01$ ;  $***p < 0.001$  vs. vehicle. **(C)**, the mRNA levels of *Il1 $\beta$* , *Il6*, and *Tnf $\alpha$*  were determined by means of qRT-PCR and normalized by means of average *Gapdh*, *Tbp*, and  *$\beta$ -actin*. The data is depicted as mean  $\pm$  SEM ( $n = 4$ ). Statistical analysis was performed with one-way ANOVA followed by the Bonferroni test to check inter-group differences.  $***p < 0.001$  vs. LPS.

### Detailed Description of the Invention

**[0018]** The present invention is illustrated by means of the following examples without the intention of limiting the scope of protection of the invention.

#### Example 1. Results.

##### Example 1.1. Computational search for $\beta$ -TrCP/NRF2 interaction inhibitors.

**[0019]** In order to find molecules capable of specifically interrupting  $\beta$ -TrCP-NRF2 interaction, a virtual analysis was carried out by means of molecular modeling and molecular dynamics tools based on the structural similarity of 388,503 natural compounds obtained from the "ZINC natural products" and the "National Center for Biotechnology Information (NCBI) PubChem database" compound libraries (**Figure 2**).

**[0020]** For this *in silico* study, the crystallographic structure PDB: 1P22 of  $\beta$ -TrCP which is published in the *Protein Data Bank* database and complexed with Skp1- $\beta$ -Catenin was used. The specific 3D preparation and editing of  $\beta$ -TrCP was performed using the tool Pymol software v 2.3.3, thereby obtaining the Skp1- and  $\beta$ -catenin-free  $\beta$ -TrCP molecule. The present group has previously characterized the most relevant moieties at the site of interaction between  $\beta$ -TrCP WD40 domain and the phosphodegron generated by GSK-3 $\beta$  in the Neh6 domain of NRF2. This NRF2 interaction site was used to identify the compounds having the highest theoretical affinity for  $\beta$ -TrCP. In this study, the AutoDock Vina tool which incorporates evolutionary and Lamarckian genetic algorithm methods, among others, has been used, allowing ligand flexibility to be modeled, while the receptor is kept rigid. Moreover, in addition to its theoretical efficacy for inhibiting  $\beta$ -TrCP-NRF2 interaction, ADMET properties (absorption, biodistribution, the speed at which it is metabolized, excretion, and toxicity) were analyzed using DataWarrior software and the ADMETSar online tool.

**[0021]** Based on the data obtained from molecular modeling, 215 compounds were selected based on their Gibbs free energy ( $\Delta G$ ), meeting the criterion of  $\leq -9.5$  kcal/mol. Then, those compounds with ADMET proper-

ties outside the established optimal ranges were eliminated. Lastly, due to the high structural homology among the 86 selected candidates, they were grouped into 39 clusters having at least 70% homology.

**[0022]** Since molecular modeling by AutoDock Vina only provides a static idea of interaction, to fine tune the selection of the best theoretical candidates, theoretical models of molecular dynamics are carried out using YASARA software. The purpose is to check whether the interactions established by the compounds selected in the first part of the process with  $\beta$ -TrCP are stable during the specific study time (100 ns). Based on these results, 4 candidates (representing 4 clusters having a different homology) with the theoretical capacity to establish stable interactions with  $\beta$ -TrCP throughout the study time were obtained.

**[0023]** By analyzing the computational parameters obtained for PHAR (**Figure 3**), the molecular modeling results showed that the compound binds to  $\beta$ -TrCP with a theoretical value of  $\Delta G = -10.35$  kcal/mol. Using the PHAR pose with the lowest free energy derived from molecular modeling, the interactions established by the compound with  $\beta$ -TrCP moieties were studied in detail, establishing as selection criterion a distance less than or equal to 3.5 Å (**Figures 3A and 3B**). The purpose was to enable evaluating the capacity of the compound to interrupt  $\beta$ -TrCP-phospho-NRF2 (pNRF2) interactions. The  $\beta$ -TrCP moieties of interest involved in the hydrophobic interactions with pNRF2 are: Arg521, Phe523, Tyr271, Arg474, Ala 434, Asn394, and Leu351. Meanwhile, the electrostatic interactions involve the following  $\beta$ -TrCP moieties: Arg285, Ser325, Lys365, Tyr438, Arg431, Asn394, and Gly408. As shown in **Figure 3A**, PHAR establishes interaction with most of the moieties involved in the hydrophobic pNRF2- $\beta$ -TrCP interaction, with the exception of Tyr271. In contrast, only interaction with Ser448, involved in electrostatic interactions, could be inhibited by PHAR. It must be pointed out that PHAR is capable of establishing interaction with more  $\beta$ -TrCP moieties other than those listed above (magenta, **Figures 3A and 3B**). This could entail the advantage of taking up more space at the site where it interacts with pNRF2, complicating the binding capacity thereof.

**[0024]** In turn, as shown in **Figure 3C**, the analysis of molecular dynamics showed that the interaction with  $\beta$ -TrCP, established by PHAR, is stable for at least 100 ns. In contrast, **Figure 3D** shows how the interaction it establishes with KEAP1 is unstable since the compound leaves the binding site during this time. Again, long-term analysis of interacting moieties corroborated, by means of molecular dynamics, that PHAR interacts with many of the moieties involved in pNRF2/ $\beta$ -TrCP interaction such as: Asn394, Gly408, Arg431, Gly432, Ser448, Leu472, Arg474, Phe523 (**Figure 3E**). With respect to ADMET predictions (**Figure 3F**), PHAR is within the optimal ranges corresponding to Lipinski's rule.

**[0025]** Therefore, computational analysis shows that PHAR could indeed interact with  $\beta$ -TrCP, but not with

KEAP1, in the key moieties of the NRF2 binding site, and could thereby compete with the binding of NRF2 to  $\beta$ -TrCP.

**Example 1.2. PHAR activates the NRF2-mediated signaling pathway.**

**[0026]** In order to empirically determine if PHAR activates NRF2, mouse embryo fibroblasts (MEFs) were treated with several doses of the compound (1  $\mu$ M, 3  $\mu$ M, and 9  $\mu$ M) for 16 h and with 10  $\mu$ M of sulforaphane (SFN), one of main electrophilic activators of NRF2, used as a positive control. PHAR induced NRF2 accumulation, although to a slightly lesser extent than the accumulation induced by SFN. This NRF2 accumulation was reflected in an increase, mainly with the dose of 9  $\mu$ M, in the levels of one of its best characterized targets: heme oxygenase-1 (HO-1) (**Figures 4A, 4B, and 4C**).

**[0027]** Moreover, a time course of NRF2 activation with PHAR (10  $\mu$ M for 2, 4, and 8 h) or with SFN (10  $\mu$ M, 8 h) was done as a positive control. PHAR induced NRF2 accumulation 2 h after treatment which was similar to the induction generated by SFN. Said accumulation correlated with the increase in HO-1 levels after 8 h (**Figures 4D, 4E, and 4F**).

**[0028]** Finally, the transcriptional activity of NRF2 was corroborated by means of luciferase assays using the reporter cell line MCF-7 c32 ARE-LUC. It is observed that PHAR (9  $\mu$ M, 16 h) produces a ~4-fold increase in luciferase activity, similar to that obtained with the positive control (SFN, 9  $\mu$ M, 16 h) (**Figure 4G**). Cell viability associated with treatment, evaluated by means of an MTT assay, demonstrated that the compound does not present toxicity at any of the doses used (**Figure 4H**). Finally, said transcriptional activity was corroborated in MEFs by means of evaluating the expression levels of several NRF2-regulated genes after treatment with PHAR (10  $\mu$ M, 8 h). The analyzed targets were *Hmox1*, *Nqo1*, *Aox1*, *Gclc*, and *Gclmy* an increase in the corresponding transcripts was observed in all the cases (**Figure 4I**).

**[0029]** As a whole, these results indicate that PHAR stabilizes NRF2 levels, and as a result increases the expression of its target genes.

**Example 1.3. PHAR activates the NRF2/HO-1 axis independently of KEAP1.**

**[0030]** From a viewpoint of biopharmaceutical usefulness, it is important to determine if PHAR acts on KEAP1/NRF2 interaction, or if it represents, in contrast, a novel approach directed specifically at  $\beta$ -TrCP/NRF2 interaction. For this purpose, MEFs originating from KEAP1 knock-out (*Keap1<sup>-/-</sup>*) and wild type (*Keap1<sup>+/+</sup>*) mice from the same litter (**Figures 5A, 5B, 5C, and 5D**) were used. NRF2 and HO-1 induction was similar in both cell lines treated with PHAR (10  $\mu$ M, 2, 4, and 8 h) (**Figures 5A, 5B, and 5C**). The same result was obtained

upon analyzing the mRNA levels of other NRF2 targets (**Figure 5D**). As an additional control, the HO-1 levels in MEFs originating from NRF2 knock-out (*Nrf2<sup>-/-</sup>*) and wild-type (*Nrf2<sup>+/+</sup>*) mice from the same litter were analyzed by immunoblot. Both cell types were incubated with PHAR (10  $\mu$ M, 2, 4, and 8 h). MEFs originating from *Nrf2<sup>+/+</sup>* mice showed a significant increase in HO-1 which was not observed in MEFs originating from *Nrf2<sup>-/-</sup>* mice (**Figures 5E and 5G**), indicating that NRF2 is essential for the induction of HO-1 by PHAR. The same result was obtained upon analyzing the mRNA levels of several NRF2 targets in both cell types (**Figure 5H**). Therefore, PHAR induces NRF2 independently of KEAP1 and said activation is responsible for the increase in the expression of its target genes.

**Example 1.4. PHAR blocks  $\beta$ -TrCP/NRF2 interaction.**

**[0031]** *In silico* studies suggested that PHAR increases NRF2 levels by means of inhibiting NPP2- $\beta$ -TrCP interaction. To confirm this, the PI3K/AKT signaling pathway is first inhibited, and therefore GSK-3 $\beta$  is activated with the PI3K inhibitor, LY294002. As a result, NRF2 is phosphorylated in its Neh6 domain and marked for degradation by means of interaction with  $\beta$ -TrCP. Therefore, if PHAR inhibits  $\beta$ -TrCP-NRF2 interaction, according to *in silico* predictions, NRF2 levels will remain stable independently of the activation and phosphorylation by GSK-3 $\beta$ . Furthermore, to once again rule out a possible KEAP1-mediated alternative mechanism, MEFs originating from *Keap1<sup>-/-</sup>* mice were used. These cells were pretreated with 10  $\mu$ M of PHAR or DMSO as a vehicle for 1 h and treatment with LY294002 (20  $\mu$ M, 15, 30, 60, 120, and 240 min) was then carried out. LY294002 caused a reduction of pSer473-AKT (by inactivating it) and pS9-GSK3 (by activating it) (**Figure 6A**), and furthermore caused a drop in NRF2 levels which can be observed mainly after 120 and 240 min of treatment. In contrast, pre-treatment with PHAR not only prevented LY294002-induced NRF2 degradation, but furthermore favored NRF2 accumulation independently of the activation of GSK3- $\beta$ / $\beta$ -TrCP (**Figures 6A and 6B**). Therefore, these results suggest that PHAR promotes NRF2 accumulation by means of inhibiting interaction with  $\beta$ -TrCP.

**[0032]** Moreover, the present group has developed NRF2 Knock-in mice (*Nrf2-2Ki*) characterized in that serines 335 and 338, which are fundamental for interaction with  $\beta$ -TrCP, have been substituted with alanines. The mutation of these two serines makes it impossible for GSK-3 $\beta$  to phosphorylate NRF2, and therefore a protein which is not recognized by  $\beta$ -TrCP, and which, accordingly, should also not be sensitive to the action of PHAR, is generated. Immortalized MEFs originating from wild-type (*Nrf2<sup>+/+</sup>*) and *Nrf2-2Ki* mice were treated with PHAR (16 h, 1  $\mu$ M, 3  $\mu$ M, and 9  $\mu$ M) or with SFN (10  $\mu$ M, 16h) as a positive control (**Figure 6C**). SFN induced potent activation of NRF2 and HO1 in both cell types as expected, since its mechanism of action is mediated by KEAP1

alone. However, PHAR-mediated activation was considerably lower in *Nrf2-2Ki* MEFs.

**[0033]** In other experiments, silencing of the two isoforms described for  $\beta$ -TrCP ( $\beta$ -TrCP1 and  $\beta$ -TrCP2) was performed in MEFs originating from *Keap1<sup>-/-</sup>* mice. Silencing was performed by means of infection with lentiviral vectors shRNA control (shCTRL) or  $\beta$ -TrCP1 and  $\beta$ -TrCP2 (sh  $\beta$ -TrCP1/2) for 5 days followed by selection of the infected cells with puromycin. Once silencing was performed, the cells were treated with PHAR (10  $\mu$ M, 2, 4, and 8h). Although the silencing achieved was about 50% for both isoforms (**Figure 6G**), this was sufficient to observe a significant increase in levels of  $\beta$ -catenin protein, used as the  $\beta$ -TrCP silencing control as it is one of its main targets (**Figure 6D**). In these conditions, it can be seen in shCTRL cells that PHAR causes an increase in NRF2 levels from 2 h to 8 h after sustained treatment. In contrast, the partial silencing of  $\beta$ -TrCP1/2 caused a slight increase in baseline NRF2 levels compared with shCTRL. However, although NRF2 accumulation occurred as a result of the treatment (probably due to the silencing achieved not being 100%), this accumulation was significantly lower compared with shCTRL cells (**Figures 6D and 6E**). Likewise, HO-1 accumulation was lower in cells lacking  $\beta$ -TrCP1/2 (**Figures 6D and 6F**). The mRNA levels corresponding to conventional NRF2 targets, *Hmox1* and *Nqo1*, confirmed the result obtained in protein, seeing that the induction generated by PHAR is lost with the silencing of both isoforms of  $\beta$ -TrCP (**Figure 6H**). Therefore, it can be concluded that the mechanism of action of the PHAR compound is mediated by its capacity to inhibit  $\beta$ -TrCP-NRF2 interaction.

#### Example 1.5. PHAR reduces inflammatory response in LPS-stimulated cells.

**[0034]** Once the mechanism of action of PHAR was deciphered, the capacity thereof to carry out protection against general lipopolysaccharide (LPS)-induced inflammation was evaluated. The NRF2/HO-1 axis contributes to inflammation resolution through direct and indirect mechanisms. Direct mechanisms include transcriptional induction of anti-inflammatory genes (MARCO, CD36), as well as transcriptional repression of pro-inflammatory genes (IL6, IL1 $\beta$ ). Indirect mechanisms involve the inhibition of reactive oxygen species and reactive nitrogen species (ROS/RNS) or of the migration/infiltration of immune cells. Furthermore, the NRF2-ARE pathway is in equilibrium with the NF- $\kappa$ B pro-inflammatory pathway.

**[0035]** First, an established mouse macrophage cell line (Raw264.7) is used and subjected to pre-treatment with a vehicle (DMSO) or PHAR (10  $\mu$ M, 8h) to obtain increased NRF2 and HO-1 levels. The cells were then stimulated with LPS (100 ng/ml, 1, 2, or 4 h) to trigger an inflammatory response. After 4 h of treatment, the LPS indeed caused an increase of several inflammatory markers: p65, pre-IL1 $\beta$ , NOS2, and COX2 (**Figures 7A and 7C**). In contrast, pretreatment with PHAR increased

NRF2 and HO-1 levels (**Figures 7A and 7B**) but, furthermore, mitigated the increase in inflammatory parameters determined by immunoblot (**Figures 7A and 7C**) or by mRNA levels (*111 $\beta$* , *Cox2*, *Nos2*) (**Figure 7D**). Furthermore, other pro-inflammatory cytokines (*Il6* and *Tnfa*) also experienced a significantly milder induction in cells pretreated with PHAR (**Figure 7E**). Therefore, PHAR reduces the inflammatory response in response to LPS in Raw264.7 cells.

**[0036]** As a complementary approach, peritoneal macrophages extracted from *Nrf2<sup>+/+</sup>* mice and *knock-in* mice generated in the laboratory having 4 serines substituted with alanines in critical positions for phosphorylation by priming kinase/priming kinases and by GSK-3 $\beta$  (Serines 335, 338, 342, and 347) were used. Both cell types were pretreated with DMSO or PHAR (10  $\mu$ M, 8h) and then stimulated with LPS (100 ng/ml, 4h). In these cell models, LPS caused an increase in inflammatory markers in peritoneal macrophages originating from *Nrf2<sup>+/+</sup>* mice (**Figure 8A left panel and Figure 8C**). Pretreatment with PHAR caused a significant increase in NRF2 and HO-1 protein levels (**Figure 8A left panel and Figure 8B**) but the production of inflammatory markers was significantly lower in those analyzed at the protein level (pre-IL1 $\beta$ , COX2, and NOS2) (**Figure 8A left panel and Figure 8C**) and mRNA level (*111 $\beta$* , *Cox2*, *Nos2*, *Il6*, and *Tnfa*) (**Figure 8D**). In peritoneal macrophages derived from 4KI (*Nrf2-4KI*) mice, NRF2 induction in response to PHAR was considerably lower. In contrast, the same HO-1 induction in response to treatment was obtained (**Figure 8A right panel, and Figure 8B**). Interestingly, the protective effect against the PHAR-mediated inflammatory response was lost in almost all the inflammatory markers analyzed both in protein (**Figure 8A right panel and Figure 8C**) in mRNA (**Figure 8D**). Therefore, considering all the results as a whole, it can be concluded that PHAR is an anti-inflammatory compound whose mechanism of action is the activation of NRF2 by interrupting the interaction thereof with  $\beta$ -TrCP.

#### Example 1.6. PHAR increases liver NRF2 protein levels.

**[0037]** Once the mechanism of action of PHAR was deciphered, the capacity thereof to induce NRF2 levels in a murine model was evaluated. C57BL/6 mice received a single intraperitoneal (IP) injection of 50 mg/kg PHAR (Tween-80 + PBS, 1:13) or 50 mg/kg of SFN (saline) as a positive control. The UV spectrum derived from the HPLC-MS study of the PHAR compound resuspended in methanol alone helped the identification of the peak associated with the compound for subsequent identification in the tissue analysis. As shown in **Figure 1A**, the PHAR UV spectrum resulted in a peak at about 6 minutes of elution with an associated mass of 555 g/mol, as expected. Taking this as a reference point, liver tissue analysis was performed to check for the presence of PHAR therein. In **Figure 9B**, the untreated mice showed two

nonspecific peaks at about 7 and 9 minutes of elution (referred to in Figure 9B with letters A and B) identified by means of UV absorbance. However, PHAR-treated mice further showed a new peak at ~4 minutes of elution (letter C). This new peak in treated mice corresponded with the presence of the compound since the mass analysis showed the existence of a mass with a value of 555 g/mol identical to the mass obtained in Figure 1A. Likewise, analysis of liver NRF2 levels showed significant NRF2 accumulation 120 min after the administration of PHAR which was very similar to the accumulation caused by SFN (Figures 9C and 9D). However, said accumulation did not result in increased HO-1 levels, presumably because the duration of treatment was too short to generate an accumulation thereof.

[0038] For this reason, C57BL/6 mice were treated daily by IP route for 5 days with 50 mg/kg of vehicle or 50 mg/kg of PHAR. A significant increase of NRF2 and HO-1 in liver (Figures 9E and 9F) was observed 120 minutes after the last administration of the compound.

#### Example 1.7. PHAR reduces inflammatory response in LPS-treated mice.

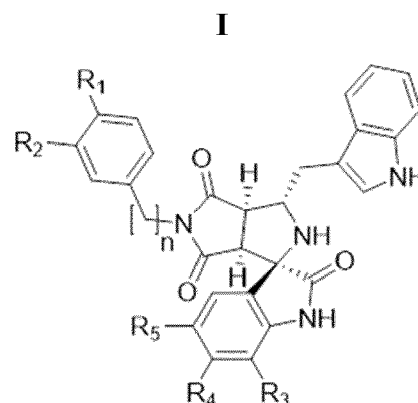
[0039] Once the *in vitro* anti-inflammatory effects of PHAR and its capacity to increase NRF2 and HO-1 levels in a model *in vivo* were demonstrated, it was evaluated whether the compound was capable of inhibiting LPS-mediated signaling in a murine model. To that end, 16 wild-type C57BL/6 mice were divided into 4 experimental groups: vehicle (experimental group 1), PHAR (experimental group 2), LPS (3), and LPS+PHAR (4). After obtaining results as promising as those described in detail in Example 1.6, the inventors decided to carry out the same experimental protocol. Briefly, the mice were treated daily by IP route with 50 mg/kg of PHAR (experimental groups 2 and 4) or vehicle (groups 1 and 3). Two hours after the second-to-last administration, experimental groups 3 and 4 were treated by IP route with 1 m/kg of LPS. Lastly, the last dose of PHAR was administered on the last day and 24 h after the administration of LPS, all the mice were sacrificed by extracting the liver protein and total RNA. Liver tissue protein analysis showed an increase in NRF2 levels derived from treatment with PHAR with a synergistic effect when treatment was performed with PHAR+LPS (Figures 10A and 10B). The clearest result was obtained when analyzing its target HO-1, where induction mediated by the compound could be clearly seen, and the same synergistic effect was again observed with combined treatment (Figures 10A and 10B). The analysis of the mRNA levels of different pro-inflammatory cytokines (*Il1 $\beta$* , *Il6*, and *Tnf $\alpha$* ) showed a significant increase as a result of treatment with LPS, as expected. In this context, prior treatment with PHAR favored a significant reduction in the production of said cytokines (Figure 10C).

[0040] Therefore, these obtained results confirm that treatment with PHAR favors an environment which pro-

ducts against inflammation in mice in response to LPS.

#### Claims

1. An NRF2- $\beta$ TrCP interaction inhibitor, characterized by Formula (I) or its derivative salts,



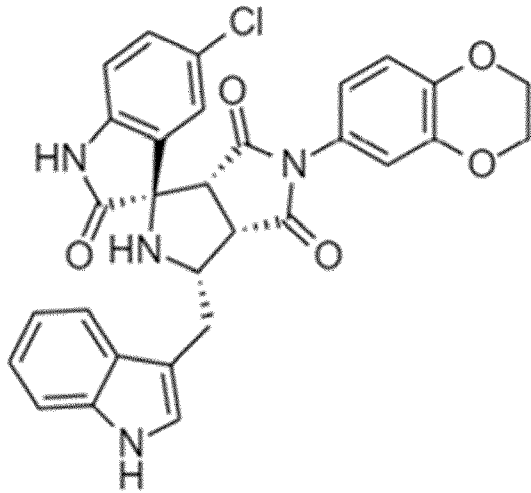
wherein:

- $n$  can be 0 or 1,
- $R_1$  can be  $O_2CCH_3$  or a six-membered ring for forming a benzodioxane, benzomethylenedioxy, or naphthalene substituent;
- $R_2$  can be H or a six-membered ring for forming a benzodioxane, benzomethylenedioxy, or naphthalene substituent;
- $R_3$  can be H or  $CH_3$ ;
- $R_4$  can be H or  $CH_3$ ; and
- $R_5$  can be H, Cl, or  $CH_3$ .

for use in the treatment of NRF2-related diseases.

2. The NRF2- $\beta$ TrCP interaction inhibitor for use according to claim 1, wherein the inhibitor is characterized by Formula (II),

**II**



or its derivative salts.

3. The NRF2- $\beta$ TrCP interaction inhibitor for use according to any of the preceding claims, in the treatment of an NRF2-related disease caused by inflammation and oxidative stress. 20
4. The NRF2- $\beta$ TrCP interaction inhibitor for use according to any of the preceding claims, in the treatment of a disease caused by Gram-negative bacterial infection. 25
5. A pharmaceutical composition comprising the NRF2- $\beta$ TrCP interaction inhibitor of Formula I or II, or derivative salts thereof, and optionally pharmaceutically acceptable vehicles or excipients, for use in the treatment of NRF2-related diseases. 30
6. The pharmaceutical composition for use according to claim 5, in the treatment of NRF2-related diseases caused by inflammation and oxidative stress. 35
7. The pharmaceutical composition for use according to any of claims 5 or 6, in the treatment of a disease caused by Gram-negative bacterial infection. 40
8. An *in vitro* method for identifying and producing compounds for the treatment of NRF2-related diseases, which comprises: a) determining if the inhibition of NRF2- $\beta$ TrCP interaction by the candidate compound has taken place, and b) wherein if said inhibition has taken place, it is indicative of the selected compound being effective in the treatment of NRF2-related diseases. 45
9. The *in vitro* method for identifying and producing compounds according to claim 8, for the treatment of NRF2-related diseases caused by inflammation and oxidative stress, which comprises: a) determining if the inhibition of NRF2- $\beta$ TrCP interaction by the candidate compound has taken place, and b) where-

in if said inhibition has taken place, it is indicative of the selected compound being effective in the treatment of NRF2-related diseases caused by inflammation and oxidative stress.

10. The *in vitro* method for identifying and producing compounds according to claims 8 or 9, for the treatment of a disease caused by Gram-negative bacterial infection, which comprises: a) determining if the inhibition of NRF2- $\beta$ TrCP interaction by the candidate compound has taken place, and b) wherein if said inhibition has taken place, it is indicative of the selected compound being effective in the treatment of a disease caused by Gram-negative bacterial infection. 50

Figure 1

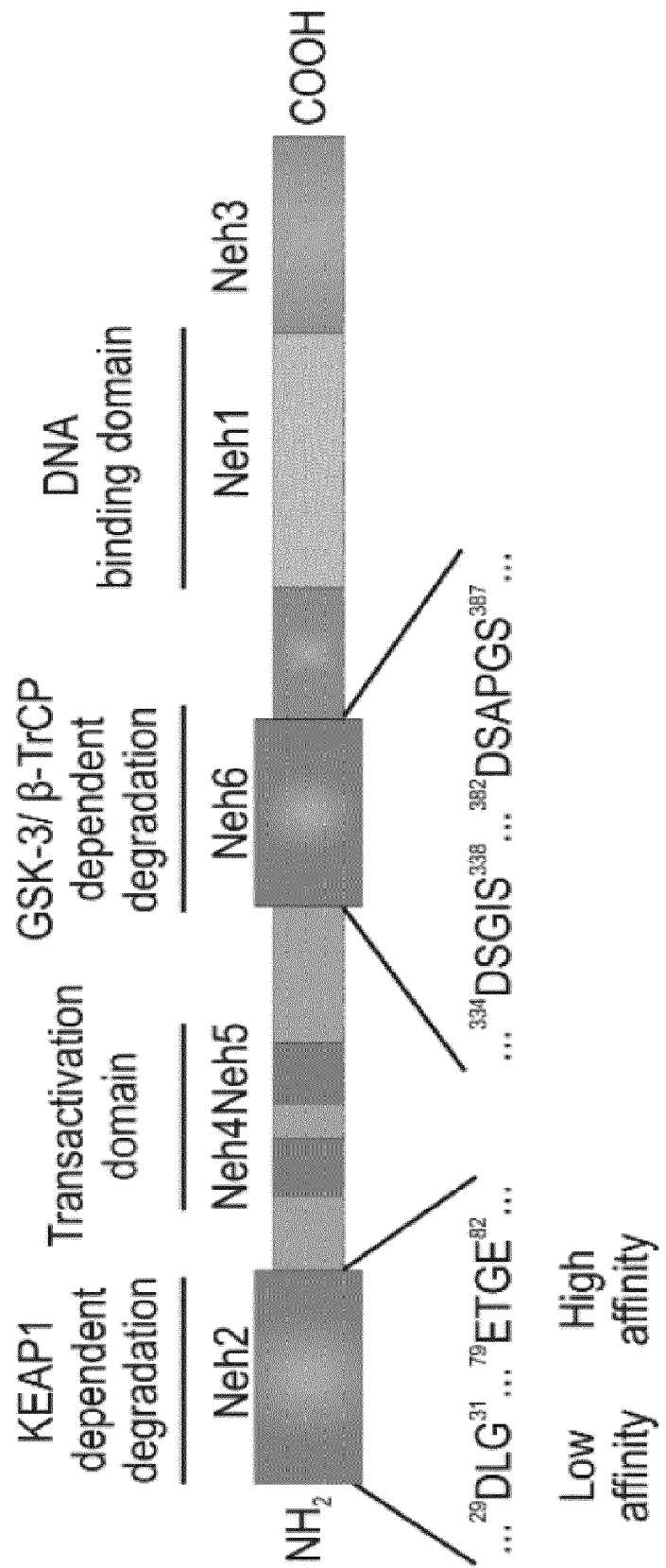


Figure 2

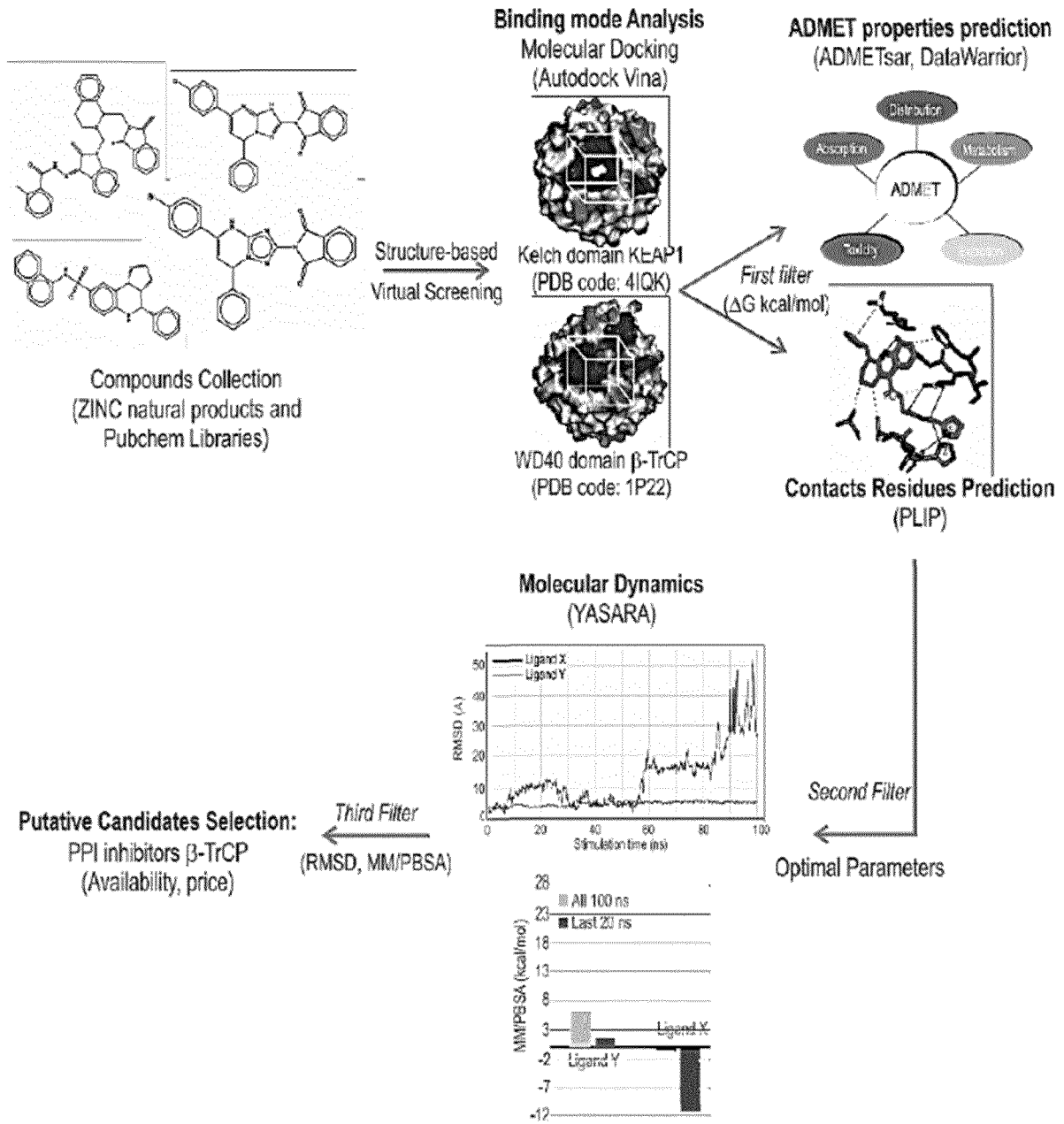


Figure 3

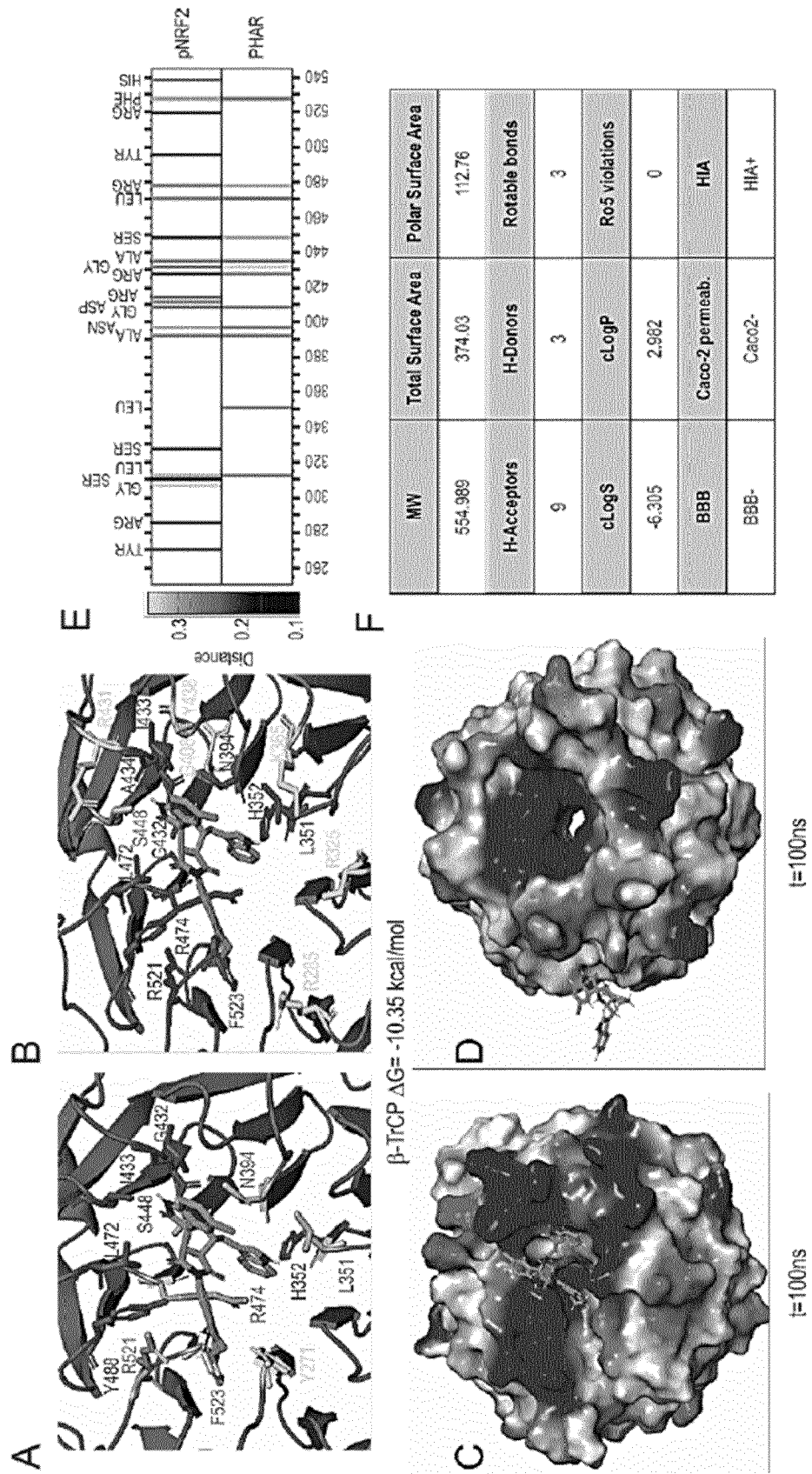


Figure 4

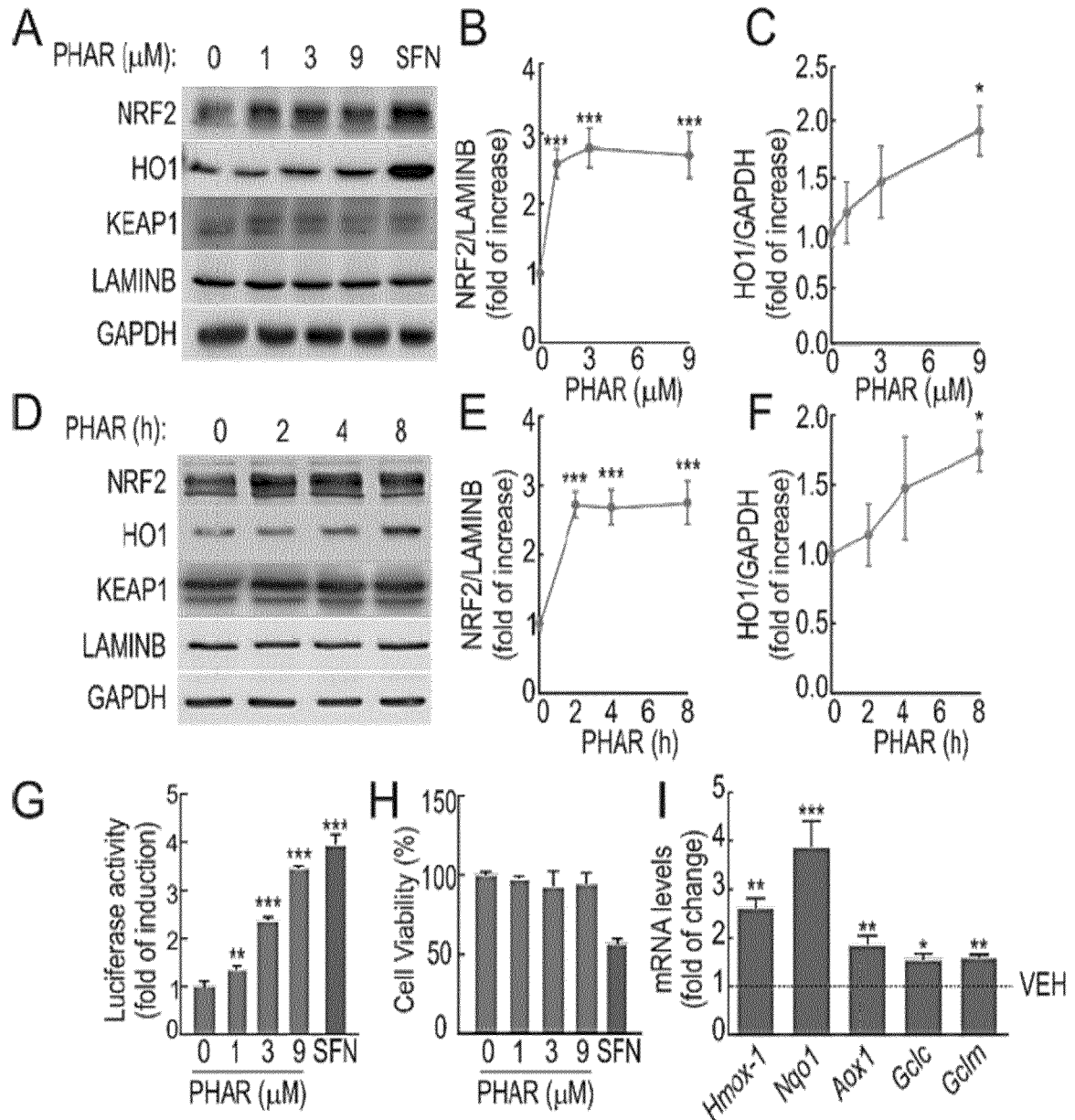


Figure 5

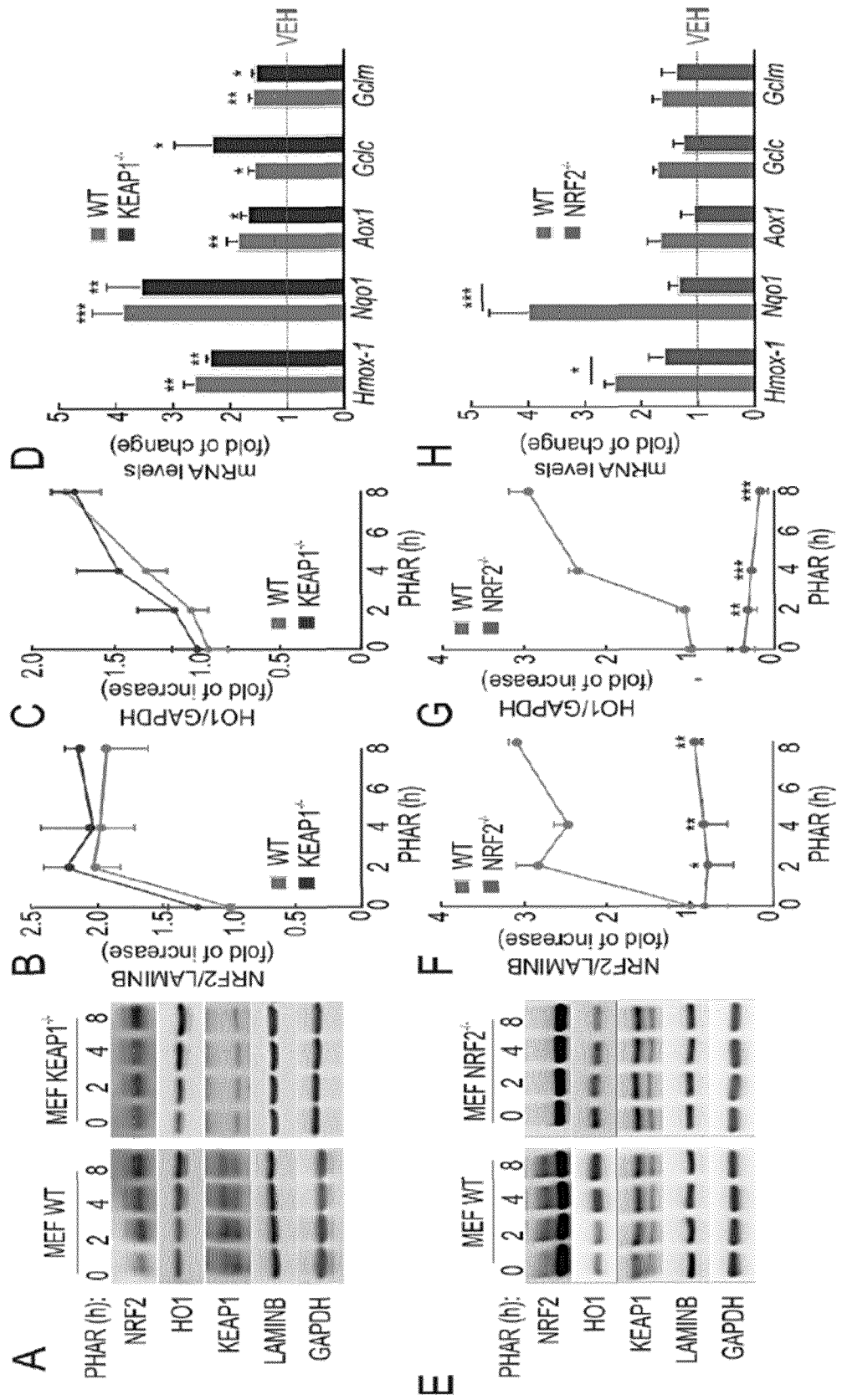


Figure 6

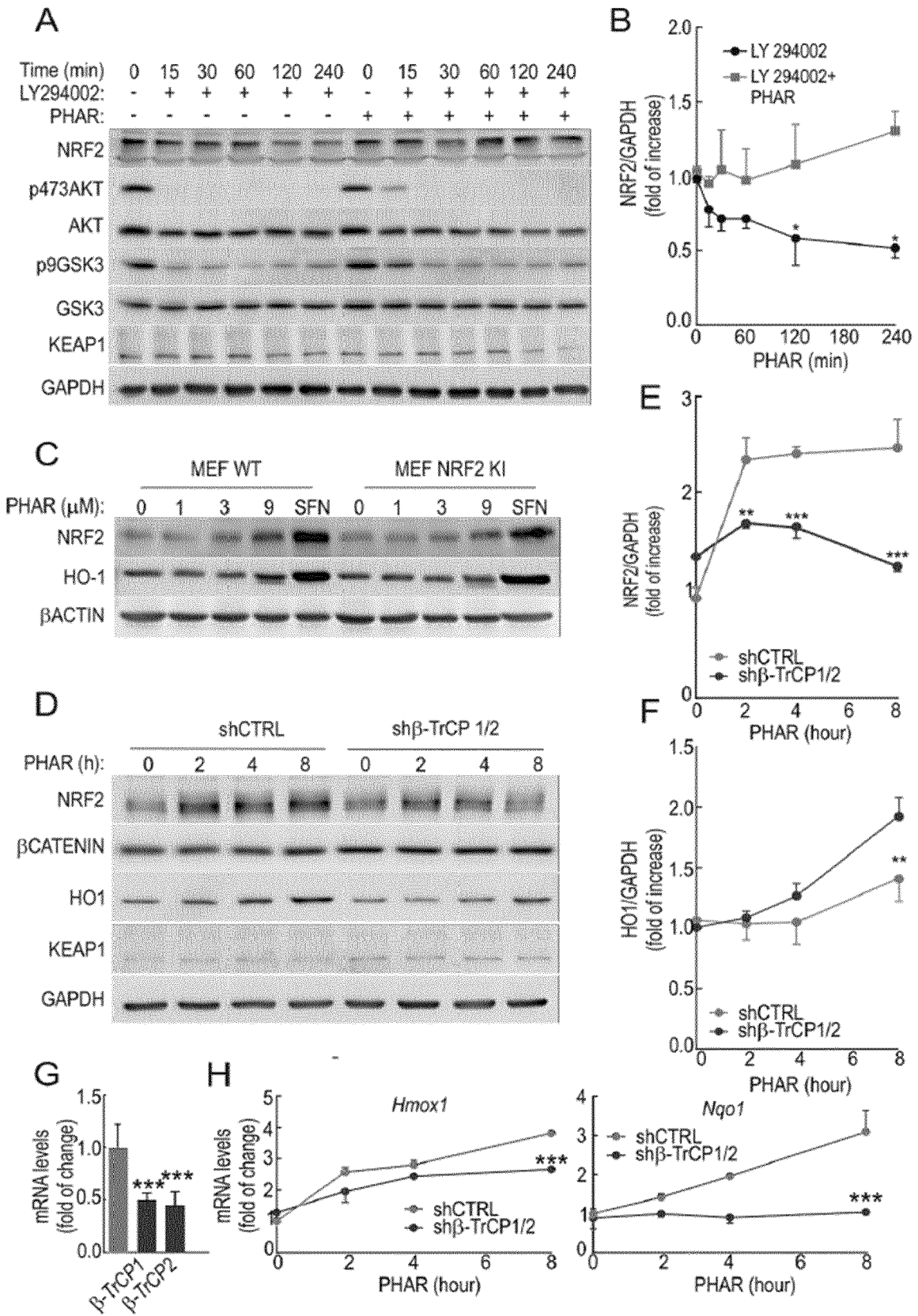


Figure 7

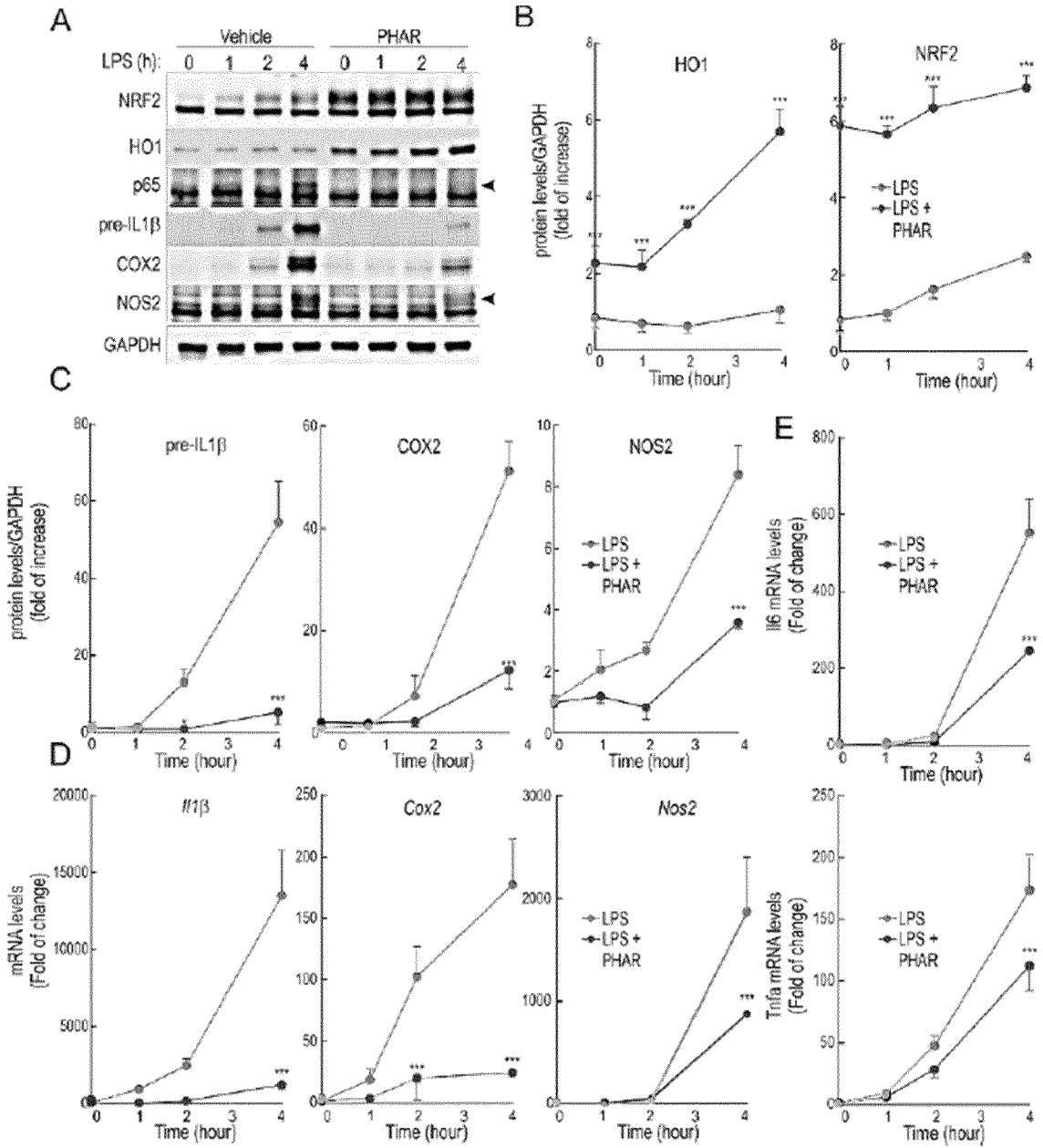


Figure 8

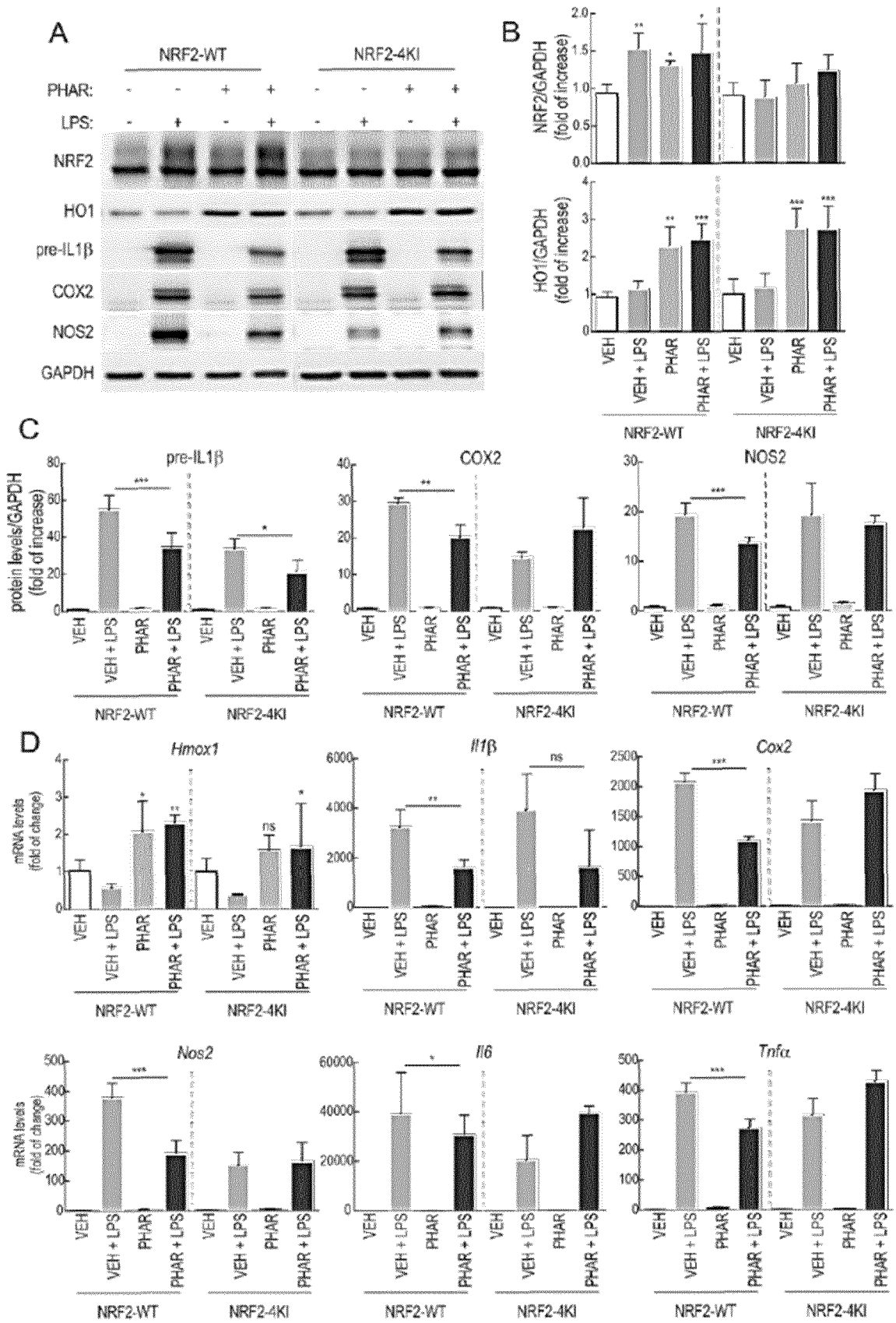


Figure 9

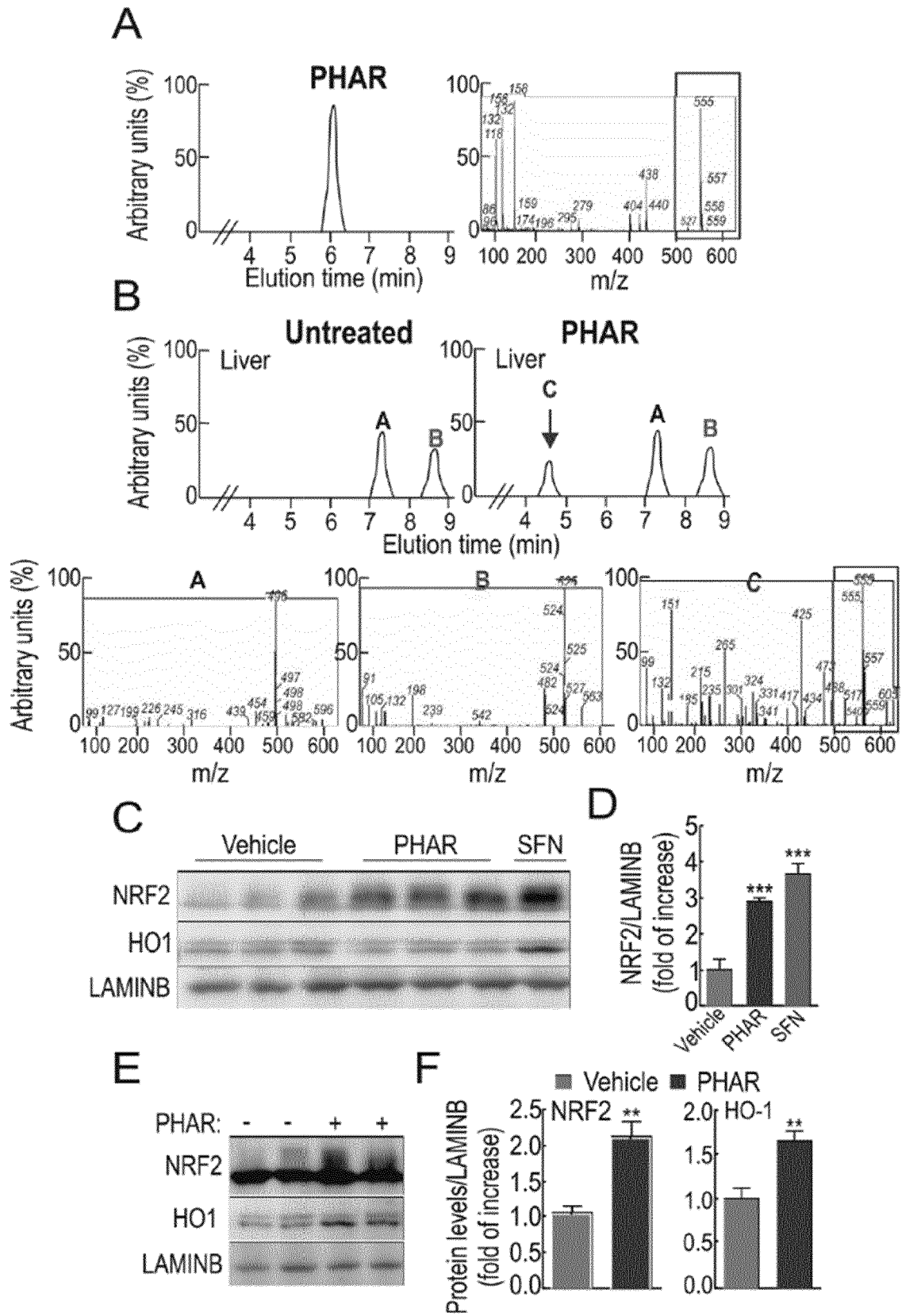
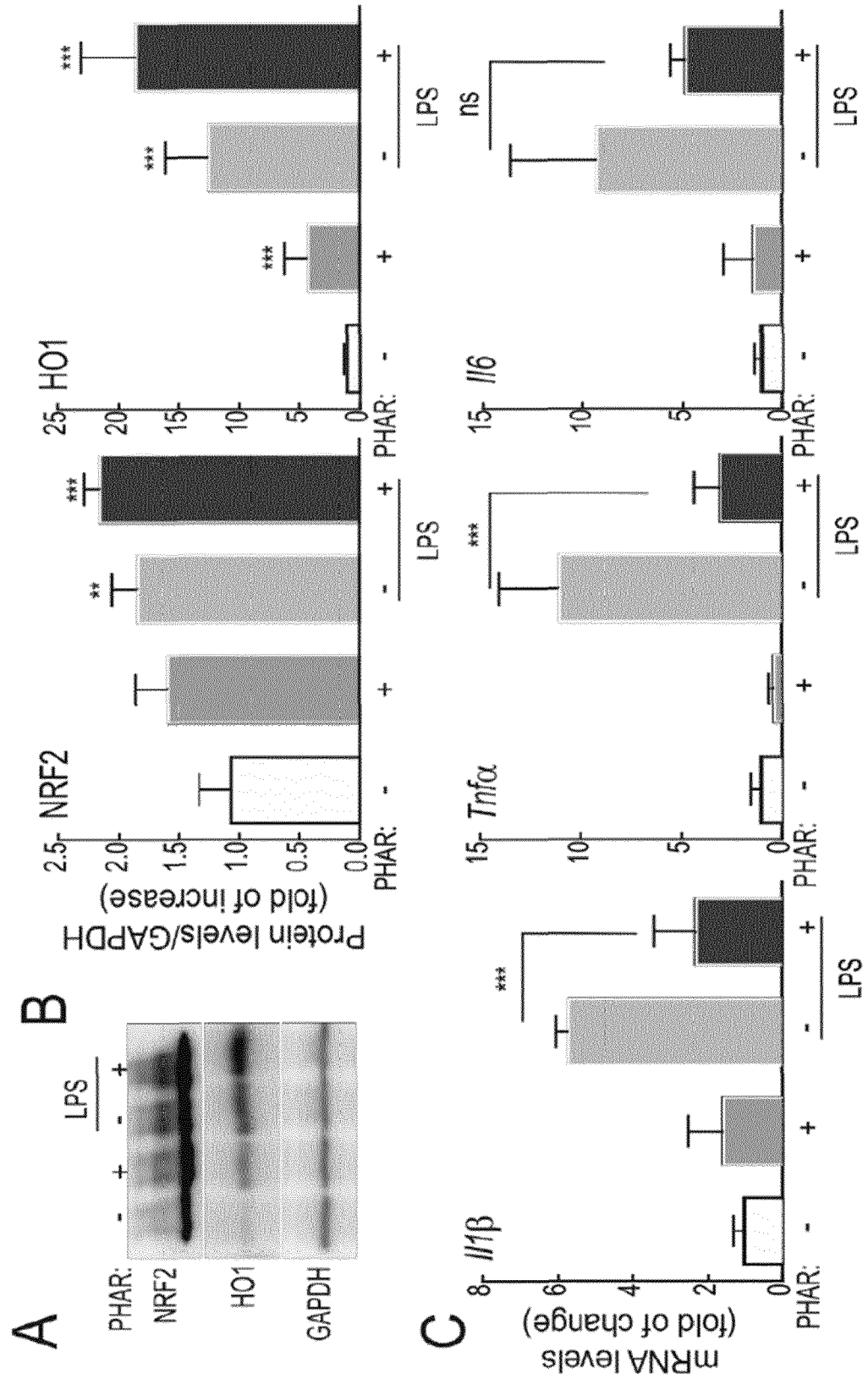


Figure 10





EUROPEAN SEARCH REPORT

Application Number  
EP 21 38 2025

5

DOCUMENTS CONSIDERED TO BE RELEVANT			
Category	Citation of document with indication, where appropriate, of relevant passages	Relevant to claim	CLASSIFICATION OF THE APPLICATION (IPC)
X	WBEIMAR ANDREY RIVERA-PÉREZ ET AL: "Molecular docking and in silico studies of the physicochemical properties of potential inhibitors for the phosphotransferase system of Streptococcus mutans", ARCHIVES OF ORAL BIOLOGY, vol. 98, 1 February 2019 (2019-02-01), pages 164-175, XP055620665, GB ISSN: 0003-9969, DOI: 10.1016/j.archoralbio.2018.09.020	1-6	INV. A61K31/404 A61P35/00 A61K31/407 A61P25/14 A61P31/04
Y	* figure 8; table 4; compound ZINC15958595 *	1-7	
Y	----- DAMALE MANOJ G. ET AL: "Molecular docking, pharmacophore based virtual screening and molecular dynamics studies towards the identification of potential leads for the management of H. pylori", RSC ADVANCES, vol. 9, no. 45, 21 August 2019 (2019-08-21), pages 26176-26208, XP055815435, DOI: 10.1039/C9RA03281A Retrieved from the Internet: URL:https://pubs.rsc.org/en/content/articlepdf/2019/ra/c9ra03281a> * figure 10 *	1-7	TECHNICAL FIELDS SEARCHED (IPC)  A61K A61P
----- -/--			
1 The present search report has been drawn up for all claims			
Place of search Munich		Date of completion of the search 21 June 2021	Examiner Bareyt, Sébastien
CATEGORY OF CITED DOCUMENTS X : particularly relevant if taken alone Y : particularly relevant if combined with another document of the same category A : technological background O : non-written disclosure P : intermediate document		T : theory or principle underlying the invention E : earlier patent document, but published on, or after the filing date D : document cited in the application L : document cited for other reasons ----- & : member of the same patent family, corresponding document	

10

15

20

25

30

35

40

45

50

55

EPO FORM 1503 03.02 (P0-C01)



## EUROPEAN SEARCH REPORT

Application Number  
EP 21 38 2025

5

10

15

20

25

30

35

40

45

50

55

DOCUMENTS CONSIDERED TO BE RELEVANT			
Category	Citation of document with indication, where appropriate, of relevant passages	Relevant to claim	CLASSIFICATION OF THE APPLICATION (IPC)
Y	SUYMKA YE. I. ET AL: "Synthesis and the antimicrobial activity of hexamethylene-Nmaleinimidospiroindole-3,3'-pyrrolo[3,4-c]pyrrole derivatives", ZHURNAL ORGANICHNOI TA FARMATSEVTICHNOI KHIMII, vol. 15, no. 4(60), 14 December 2017 (2017-12-14), pages 56-62, XP055815451, RU ISSN: 2308-8303, DOI: 10.24959/ophcj.17.929 * table 2 *	1-7	
A	----- WO 2016/201440 A1 (UNIV CALIFORNIA [US]) 15 December 2016 (2016-12-15) * claim 1; figure 6 *	1-7	
A	----- PREMACHANDRA ILANDARI DEWAGE UDARA ANULAL ET AL: "Potent Synergy between Spirocyclic Pyrrolidinoindolinones and Fluconazole against Candida albicans", CHEMMEDCHEM COMMUNICATIONS, vol. 10, no. 10, 12 August 2015 (2015-08-12), pages 1672-1686, XP055815412, DE ISSN: 1860-7179, DOI: 10.1002/cmdc.201500271 * table 1 *	1-7	TECHNICAL FIELDS SEARCHED (IPC)
A	----- CN 105 412 089 B (BEIJING COMPUTING CENTER) 1 June 2018 (2018-06-01) * claim 1; compound VS1 *	1-7	
			-/--
The present search report has been drawn up for all claims			
Place of search <b>Munich</b>		Date of completion of the search <b>21 June 2021</b>	Examiner <b>Bareyt, Sébastien</b>
CATEGORY OF CITED DOCUMENTS X : particularly relevant if taken alone Y : particularly relevant if combined with another document of the same category A : technological background O : non-written disclosure P : intermediate document		T : theory or principle underlying the invention E : earlier patent document, but published on, or after the filing date D : document cited in the application L : document cited for other reasons ..... & : member of the same patent family, corresponding document	

EPO FORM 1503 03.82 (P04C01)



EUROPEAN SEARCH REPORT

Application Number  
EP 21 38 2025

5

DOCUMENTS CONSIDERED TO BE RELEVANT			
Category	Citation of document with indication, where appropriate, of relevant passages	Relevant to claim	CLASSIFICATION OF THE APPLICATION (IPC)
A	<p>GUO RONG ET AL: "Discovery of ERBB3 inhibitors for non-small cell lung cancer (NSCLC) via virtual screening", JOURNAL OF MOLECULAR MODELING, SPRINGER BERLIN HEIDELBERG, BERLIN/HEIDELBERG, vol. 22, no. 6, 17 May 2016 (2016-05-17), pages 1-9, XP035973145, ISSN: 1610-2940, DOI: 10.1007/S00894-016-3007-Z [retrieved on 2016-05-17] * table 1; compounds VS1, VS3 *</p> <p>-----</p>	1-7	<p>TECHNICAL FIELDS SEARCHED (IPC)</p>
A	<p>ZHANG YONGTAO ET AL: "Isorhynchophylline enhances Nrf2 and inhibits MAPK pathway in cardiac hypertrophy", NAUNYN-SCHMIEDEBERG'S ARCHIVES OF PHARMACOLOGY, SPRINGER, DE, vol. 393, no. 2, 5 September 2019 (2019-09-05), pages 203-212, XP037170273, ISSN: 0028-1298, DOI: 10.1007/S00210-019-01716-0 [retrieved on 2019-09-05] * compound Isorhynchophylline *</p> <p>-----</p>	1-10	
X	<p>ZHANG DONNA D. ET AL: "The role of natural products in revealing NRF2 function", NATURAL PRODUCT REPORTS, vol. 37, no. 6, 24 June 2020 (2020-06-24), pages 797-826, XP055816013, GB ISSN: 0265-0568, DOI: 10.1039/C9NP00061E Retrieved from the Internet: URL:https://pubs.rsc.org/en/content/articlepdf/2020/np/c9np00061e&gt; * paragraph [0008] *</p> <p>-----</p> <p style="text-align: center;">-/--</p>	8,9	
<p>The present search report has been drawn up for all claims</p>			
Place of search <b>Munich</b>		Date of completion of the search <b>21 June 2021</b>	Examiner <b>Bareyt, Sébastien</b>
<p>CATEGORY OF CITED DOCUMENTS</p> <p>X : particularly relevant if taken alone Y : particularly relevant if combined with another document of the same category A : technological background O : non-written disclosure P : intermediate document</p>		<p>T : theory or principle underlying the invention E : earlier patent document, but published on, or after the filing date D : document cited in the application L : document cited for other reasons</p> <p>..... &amp; : member of the same patent family, corresponding document</p>	

EPO FORM 1503 03.02 (P04C01)

10

15

20

25

30

35

40

45

50

55



EUROPEAN SEARCH REPORT

Application Number  
EP 21 38 2025

5

DOCUMENTS CONSIDERED TO BE RELEVANT			
Category	Citation of document with indication, where appropriate, of relevant passages	Relevant to claim	CLASSIFICATION OF THE APPLICATION (IPC)
X	Zhang Di ET AL: "A novel Nrf2 inhibitor suppresses proliferation and enhances the sensitivity of cancer cells to chemotherapy", AACR-NCI-EORTC International Conference on Molecular Targets and Cancer Therapeutics, 26 October 2019 (2019-10-26), page C063, XP055816008, DOI: 10.1158/1535-7163.TARG-19-C063Published Retrieved from the Internet: URL:https://dx.doi.org/10.1158/1535-7163.TARG-19-C063Published [retrieved on 2021-06-21] * the whole document *	8,9	
X	CHOI E-J ET AL: "A clinical drug library screen identifies clobetasol propionate as an NRF2 inhibitor with potential therapeutic efficacy in KEAP1 mutant lung cancer", ONCOGENE, vol. 36, no. 37, 1 September 2017 (2017-09-01), pages 5285-5295, XP055816037, London ISSN: 0950-9232, DOI: 10.1038/onc.2017.153 Retrieved from the Internet: URL:https://www.nature.com/articles/onc2017153.pdf> * the whole document *	8,9	
			TECHNICAL FIELDS SEARCHED (IPC)
The present search report has been drawn up for all claims			
Place of search Munich		Date of completion of the search 21 June 2021	Examiner Bareyt, Sébastien
CATEGORY OF CITED DOCUMENTS X : particularly relevant if taken alone Y : particularly relevant if combined with another document of the same category A : technological background O : non-written disclosure P : intermediate document		T : theory or principle underlying the invention E : earlier patent document, but published on, or after the filing date D : document cited in the application L : document cited for other reasons & : member of the same patent family, corresponding document	

10

15

20

25

30

35

40

45

1  
EPO FORM 1503 03.82 (P04C01)

50

55



EUROPEAN SEARCH REPORT

Application Number  
EP 21 38 2025

5

DOCUMENTS CONSIDERED TO BE RELEVANT			
Category	Citation of document with indication, where appropriate, of relevant passages	Relevant to claim	CLASSIFICATION OF THE APPLICATION (IPC)
X	GUNNE SANDRA ET AL: "Nrf2-A Molecular Target for Sepsis Patients in Critical Care", BIOMOLECULES, vol. 10, no. 12, 17 December 2020 (2020-12-17), page 1688, XP055816065, DOI: 10.3390/biom10121688 * the whole document * -----	8-10	
			TECHNICAL FIELDS SEARCHED (IPC)
The present search report has been drawn up for all claims			
Place of search <b>Munich</b>		Date of completion of the search <b>21 June 2021</b>	Examiner <b>Bareyt, Sébastien</b>
CATEGORY OF CITED DOCUMENTS X : particularly relevant if taken alone Y : particularly relevant if combined with another document of the same category A : technological background O : non-written disclosure P : intermediate document		T : theory or principle underlying the invention E : earlier patent document, but published on, or after the filing date D : document cited in the application L : document cited for other reasons ..... & : member of the same patent family, corresponding document	

EPO FORM 1503 03.82 (P0-C01)

10

15

20

25

30

35

40

45

50

55

**ANNEX TO THE EUROPEAN SEARCH REPORT  
ON EUROPEAN PATENT APPLICATION NO.**

EP 21 38 2025

5

This annex lists the patent family members relating to the patent documents cited in the above-mentioned European search report. The members are as contained in the European Patent Office EDP file on  
The European Patent Office is in no way liable for these particulars which are merely given for the purpose of information.

21-06-2021

10

Patent document cited in search report	Publication date	Patent family member(s)	Publication date
WO 2016201440 A1	15-12-2016	US 2020140449 A1 WO 2016201440 A1	07-05-2020 15-12-2016
-----	-----	-----	-----
CN 105412089 B	01-06-2018	NONE	
-----	-----	-----	-----

15

20

25

30

35

40

45

50

55

EPO FORM PC459

For more details about this annex : see Official Journal of the European Patent Office, No. 12/82

**REFERENCES CITED IN THE DESCRIPTION**

*This list of references cited by the applicant is for the reader's convenience only. It does not form part of the European patent document. Even though great care has been taken in compiling the references, errors or omissions cannot be excluded and the EPO disclaims all liability in this regard.*

**Non-patent literature cited in the description**

- **ANTONIO CUADRADO et al.** Transcription Factor NRF2 as a Therapeutic Target for Chronic Diseases: A Systems Medicine Approach. *Pharmacological Reviews*, April 2018, vol. 70 (2), 348-383 [0006] [0016]